

CONSTRUCTION VERIFICATION OF AN ASYMMETRIC ARCH BRIDGE BASED ON CONSTRUCTION MONITORING AND TESTS

Xilong Zheng¹, Dachao Li², Kexin Zhang², Xiaojie Xue³ and Fanhua Min⁴

- 1. School of Civil and Architectural Engineering, Harbin University, No.109 Zhongxing Road, Harbin, Heilongjiang Province, China; sampson88@126.com*
- 2. School of Transportation and Geomatics Engineering, Shenyang Jianzhu University, No. 25 Hunnan Zhong Road, Shenyang, Liaoning Province, China; jt_zkx@sjzu.edu.cn*
- 3. Engineering Department, Guangzhou Expressway Co., LTD, No. 17 Fenghuang San Road, Guangzhou, Guangdong Province, China*
- 4. Research and Development Center, Liaoning Transportation Planning and Design Institute Co. LTD, No. 42 Lidao Road, Shenyang, Liaoning Province, China*

ABSTRACT

For the three-span continuous tied arch bridge with unequal span, its sagittal span ratio is different, which leads to the design internal force and construction is very complicated. The construction method and installation sequence are closely related to the main beam, arch rib alignment and the internal force state of the structure. For the arch bridge with special structure, the stiffness of the arch ring and the stress of the main beam will affect the stability and deformation of the whole structure. The theoretical and practical deviations of arch bridge construction are cumulative. If not timely and effective control and adjustment according to the actual data, it will endanger the safety of the structure in the construction process. In order to ensure the safety of the bridge construction process, the stress of the main beam, the centring of the arch ring and the temperature are monitored and recorded during the whole construction process. After the completion of the bridge construction, static and dynamic load tests were conducted to verify whether the bridge can meet the design specifications. The construction monitoring results indicated that during the construction of the arch bridge, the stress of the girders was in good agreement with the theoretical values, meeting the design standards and specifications. The actual alignment of arch rings was basically consistent with the theoretical alignment.

KEYWORDS

Tied arch bridge, Through arch bridge, Construction monitoring, Construction verification, Load tests

INTRODUCTION

Arch bridge is a common bridge type, which has a long history in the world. Compared to the beam bridge, the arch bridge is not only beautiful in shape, but also has greater spanning capacity. An arch bridge transmits vertical loads to its arches, which in turn transmits forces to the foundations on either side. The span of arch bridge is restricted by material properties as a flexural component [1-3]. With the progress of the times, the traditional masonry arch bridge was gradually replaced by

reinforced concrete arch bridge. The reinforced concrete (RC) arch bridge has great difficulty in construction method and construction monitoring because of its large dead weight. Tied arch bridges have the general characteristics of arch bridges as well as their own unique characteristics. It is a bridge type that combines the advantages of arch and beam. It combines the two basic structural forms of arch and beam to bear load together. This kind of arch bridge is a statically indeterminate system in the interior and a statically indeterminate system in the exterior. This structural form gives full play to the structural performance and combination function of beam bending and arch compression. The horizontal thrust at the arch end is borne by tension rod, so that the support at the arch end does not generate horizontal thrust [4-5]. Besides, it has two characteristics of large span capacity and strong adaptability to the foundation [6-7]. When the deck elevation is limited, the tied arch bridge can ensure a large clearance under the bridge [8].

As a kind of non-thrust combined system, arch rings stiffness and girders stress of the tied arch bridge will affect the stability and deformation calculation results of the whole bridge structure. The theoretical and practical deviations of arch bridges in construction are cumulative. If it is not controlled and adjusted timely and effectively according to the actual data, it will endanger the safety of the structure during the construction process. Therefore, arch bridge construction monitoring is especially essential [9-11]. The goal of load test is to measure the stress and deflection of the control section of the bridge span structure under the action of test load through the static load, and compare with the theoretical calculation value, to check whether the stress value and deflection value of the control section of the structure are consistent with the design requirements, and to evaluate the current bearing capacity of the bridge span structure. Through the dynamic load test, the overall dynamic performance of the structure and the dynamic performance under the vehicle are evaluated, which provides the original data for the bridge maintenance, management, reinforcement and repair or reconstruction in the future [12-14].

To ensure the safety construction, in the construction monitoring, the arch rings line and stress, the temperature changes before and after the girders pouring were monitored. At the same time, bridges were also experimented with static and dynamic load tests to verify whether the bridge could achieve the designed requirements. This work can offer significant reference for the construction and design of similar tied arch bridges.

BACKGROUND

Wolong River Bridge is located in Dalian City, across the Wolong River, the central axis of the bridge and the river oblique. Wolong River Bridge is a three-span continuous girder arch composite bridge. The vertical section of the completed bridge is shown in Figure 1. It has a total length of 130 m with three spans. The length of each span is 48 m, 43 m and 38.5 m respectively. The width of the bridge deck is 6.0 m (sidewalk) +11.5 m (motor vehicle lane) +4.0 m (cables area) +11.5 m (motor vehicle lane) +6.0 m (sidewalk) = 39 m. The design base period of the bridge structure is 100 years. The design of the bridge's automobile load is highway level one according to Chinese regulations. The upper column of the bridge tower adopts rectangular section, the lower column adopts cylindrical section, and the foundation adopts pile group.



Fig. 1 – Vertical section of Wolong River Bridge

The load-bearing structure consists of five rooms RC box-girders. The box-girder height at the fulcrum is increased to 3.0 m. The edge fulcrum is raised in a straight line, and the girder height in the middle fulcrum is changed in a circular arc. The top edge of the main girder within the 4 m cables area at both ends of the arch feet is increased by 0.4 m C50 concrete is used. Bridge's elevation is shown in Figure 2. The box-girder is 39 m of top width and 26.85 m of bottom width. The bi-directional 1.5% transverse slope of the deck is adjusted by the height change of the main girder web. The hanger rods are arranged within the range of the middle box, and the main girder is set with transverse diaphragms at each anchorage point of the hanger rods, the width of which is 0.35~0.65 m. Prestressed steel beams are arranged in the longitudinal and transverse beam, end beam and middle beam of the main beam. The arch axis equation is a parabolic equation, and the ratio of vector to span is $F/L = 1/1.9, 1/2.7$ and $1/3.9$, respectively. The height of the vector is about 25 m, 16 m and 10 m respectively. The section width of the arch rings is 3 m, and the height of the three spans is 1.5 m, 1.35 m and 1.2 m, respectively. The arch rings are made of C50 concrete with cast-in-place supports. PES7-55 and PES7-73 normal suspenders are used for the suspenders. The distance between the suspenders is 3.5 m, the safety factor of the suspenders is 2.5, and the tension of the single suspenders is 900 kN~1500 kN. The pile foundation is made of bored pile with a diameter of 150 cm, and the whole bridge has a total of 32 piles.

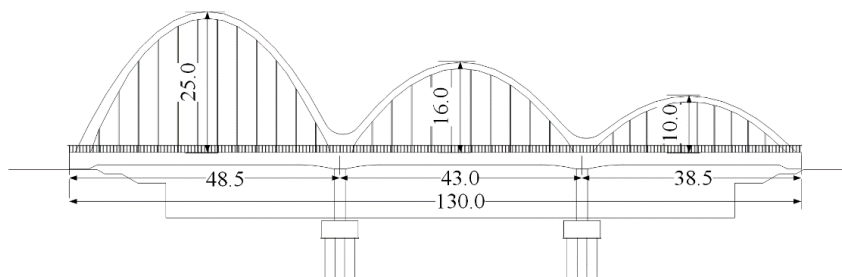


Fig. 2 – Elevation of the arch bridge (unit: m)

The construction process is mainly in group of six steps: (1) Substructure and foundation construction; (2) Set up the main girder support and cast the main girder; (3) Set up arch rings support and pour arch rings; (4) Install the suspender, tension the suspender for the first time, and remove the arch rings support; (5) Remove the main beam bracket and tension the suspender for the second time; (6) Bridge deck construction, boom force adjustment. The specific construction steps are shown in Figure 3.

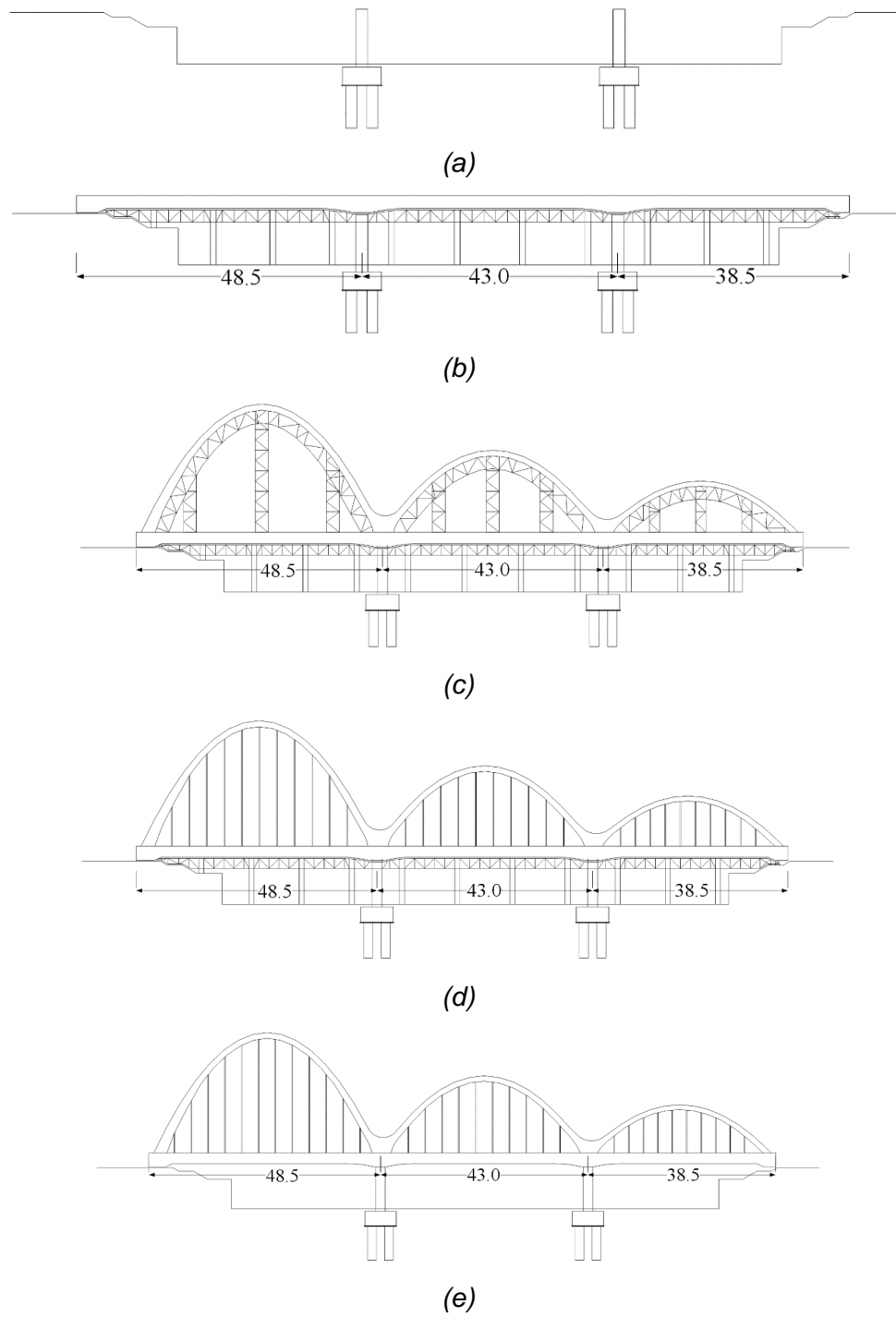
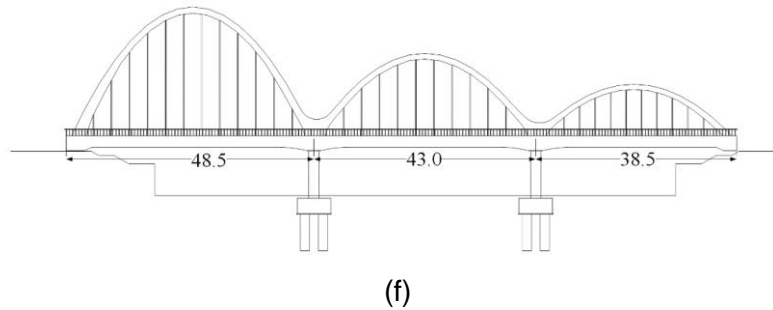


Fig. 3 – The specific construction steps



(f)
 Fig. 3 – The specific construction steps: (a) Step 1: Substructure and foundation construction; (b) Step 2: Set up the girders brackets and cast the main girder; (c) Step 3: Set up arch rings support and pour arch rings; (d) Step 4: Install the hangers, tension the hangers for the first time, and remove the arch rings support; (e) Step 5: Remove the brackets and tension the hangers for the second time; (f) Step 6: Bridge deck construction, hangers force adjustment

CONSTRUCTION MONITORING AND LOAD TEST

Continuous beam arch composite bridge presents excellent and stable economic indicators and beautiful appearance which is more suitable for soft soil foundation because of its light structure and no horizontal thrust outside [15-16]. The main arch bears the vertical load and the vertical cable force of the bridge span. This is mainly because the design parameters used in the design, such as the elastic modulus of materials, the dead weight of components and the temporary load of construction, are not completely consistent with the parameters in the actual project. The construction of complex bridge is a systematic project. In the system design is the ideal target, and from start to completion of the whole to achieve goals, the design must go through the process, will be a lot of determination and the influence of the uncertainty, including design calculation, material properties and construction precision, load, atmospheric temperature, and many other aspects of the differences between ideal state and actual state. How to find out the relative true value from various parameters distorted by errors in construction and carry out real-time identification (monitoring), adjustment (correction) and prediction of the construction state is crucial to the realization of the design goal [17-18].

Finite element model (FEM)

As a software widely used in civil engineering, Midas/Civil is adopted to build the FEM of the arch bridge. In order to facilitate the calculation, some elements in the model are simplified on the basis of fully considering the construction sequence and the structure stress. Box-girders and arch rings are girder elements, and the suspender is tensile structural elements. Figure 4 shows the FEM of the tied arch bridge.

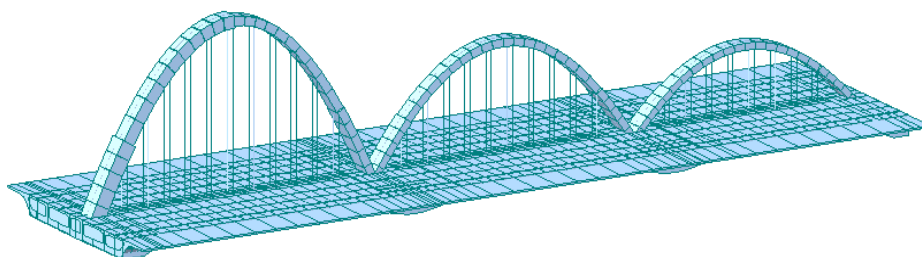


Fig. 4 – FEM of the tied arch bridge

The definition of mechanical properties of different sections of pedestrian arch bridge in the FEM is shown in Table 1. The box girders and arch rings are casted with C50 concrete. The cap and abutment are made of C40 concrete, the pier and foundation are made of C30 concrete, and the elastic modulus $E = 3 \times 10^4$ MPa. The sling is composed of 61 high-strength steel wires with a tensile strength of 1670 MPa. The standard yield strength of ordinary steel bar is 335 MPa.

Tab. 1 - Mechanical Properties Defined in the FEM

Structural Parts	Material	Compressive Strength (MPa)	Tensile Strength (MPa)	Modulus of Elasticity (MPa)
Box Girders, Arch Rings	C50 Concrete	22.4	1.83	3.45×10^4
Bridge Abutments	C40 Concrete	18.4	1.65	3.25×10^4
Bridge Piers, Foundation	C30 Concrete	13.8	1.39	3.00×10^4
Suspenders	OVM.PES7-61	-	1670	2.05×10^3
Prestressed Reinforcement	$\Phi 15.2$ Steel Strand	-	1860	-
Steel Bars	HRB335	-	420	2.10×10^5

Construction monitoring scheme

Position of measuring points

As shown in Figure 5, six test sections are arranged in the arch bridge. Concrete temperature measurement is to test and monitor the temperature distribution of the whole pouring block, to provide guidance for construction.

Measuring point arrangement of arch rings elevation is shown in Figure 6. Elevation observation should be carried out in 33 sections where the arch rings, arch foot and suspender are located. Therefore, there are 66 measuring points in the whole elevation. Permanent observation points are set up at the top and foot of the arch. The data of these observation points are one of the most important data in construction monitoring.

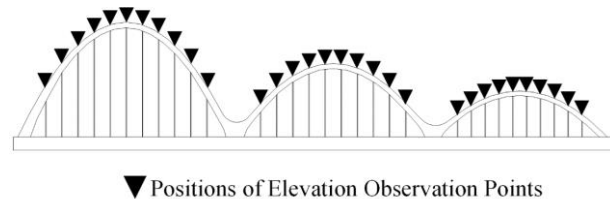
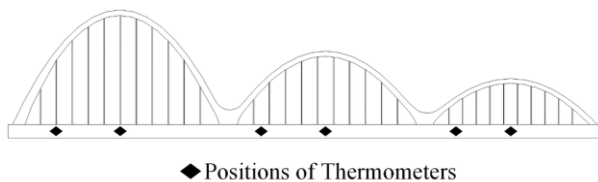


Fig. 5 – Positions of measuring points Fig. 6 – Measuring points for elevation of arch rings

Static load tests

Test contents

Based on the stress characteristics of the tied arch bridge, test sections are determined as the

1/2, 1/4, 1/8, 3/4, and 7/8 span section. The test content and measuring points are shown in Table 2. Static load tests include vertical deflection, longitudinal displacement and strains of the girders. In addition, the hangers force is also tested in the experiments. The placement of measuring points in this static load test is shown in Figure 7.

Tab. 2 - Test Contents of Static Load Tests

Measuring Points	Test Contents
N1-N6	Deflection of Girder
M1-M6	Lateral Strain of Girder
M7-M12	Vertical Strain of Girder
D1-D3	Hangers Force

Arrangement of test vehicles and measuring points

The layout of measuring points in static load test is shown in Figure 7. If the actual load of the vehicle is inconsistent with the calculation and analysis, it will be adjusted in the later stage. The test vehicles are planned to be 6 trucks each weighing 450kN, and the specific parameters are shown in Table 3.

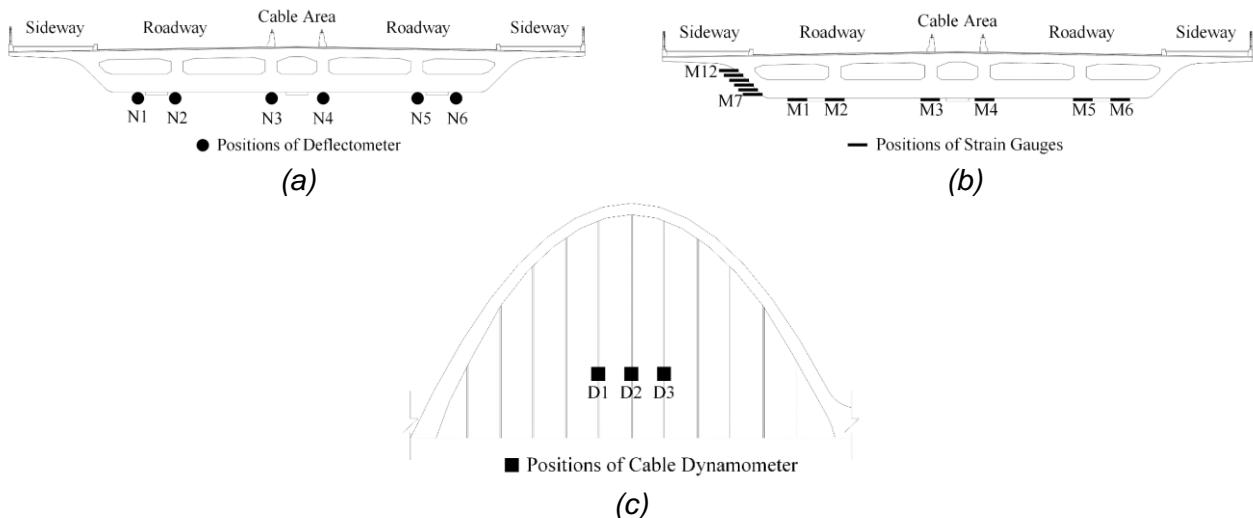


Fig. 7 – The layout of measuring points in static load test :(a) Deflection measurement points;(b) Strain measuring points; (c) Hangers force measuring points

Tab. 3 - Detailed Data of The Loading Vehicle

P1	P2	P3	A	B	C	D
Front Axle	Rear 1Axis	Rear 2 Axis	Wheelbase	Wheelbase	Wheelbase	Wheelbase
(kN)	(kN)	(kN)	(cm)	(cm)	(cm)	(cm)
40~80	90~130	90~130	130~145	330~430	300~500	180

The static test load loading method is to use the three-axle truck as the equivalent load. Meanwhile, the equivalent load can generate the stress in the test process. Therefore, for a specific

of the real bridge structures are often complex, are generally not random, directly according to the signal or data to analyze and judge the regularity of structural vibration is difficult, usually need to analyze the vibration waveform and processing, in order to do further analysis for structure dynamic performance, can draw such as amplitude, parameters such as damping ratio, coefficient of vibration mode, impact [19-23]. Frequency domain analysis is to reveal the frequency of the signal components and transfer characteristics of vibration system. Then the distribution of vibration energy can be found by frequency, so as to determine the frequency and frequency distribution characteristics of the bridge. It is concluded that the vibration quantity after, can be in accordance with the relevant index comprehensive evaluation of the dynamic properties of bridge structure. The layout of dynamic load test points is shown in Figure 9. Bridge dynamic load test adopts the bridge dynamic data acquisition system produced by Donghua Test Technology Co., LTD. The acquisition system model is DH5937.

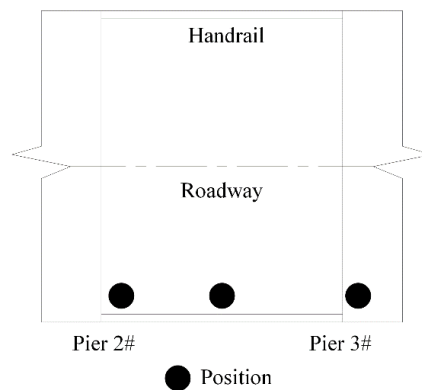
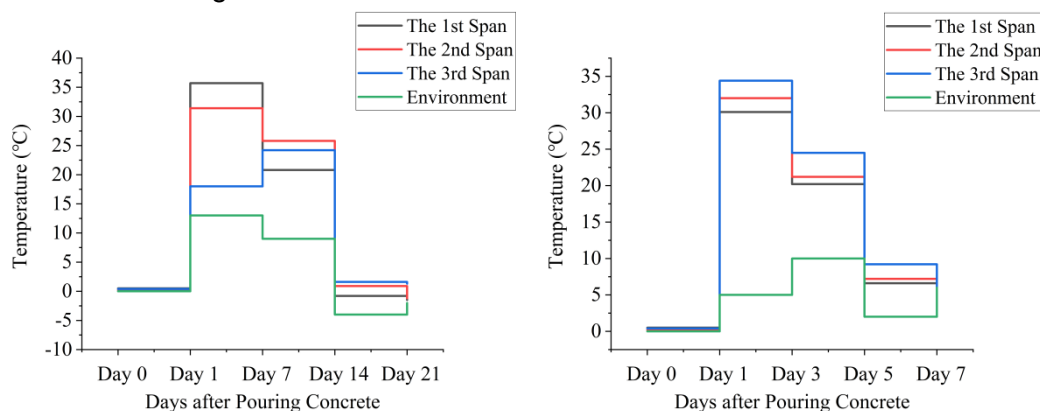


Fig. 9 – Layout of dynamic load test points

CONSTRUCTION MONITORING RESULTS

Temperature monitoring results

The test results of temperature monitoring are shown in Figure 10. The observed maximum temperature of the main girder can reach 34.4 °C and the lowest temperature is 0.2 °C; the observed maximum temperature of the roof can reach 38.1 °C and the lowest temperature is -3.8 °C. The temperature change trend is very regular after the girders concrete poured. After the arch rings concrete poured, the temperature of the tied arch bridge varied within a reasonable range. The temperature changes of the whole bridge are in accordance with the natural conditions, and the structure of the whole bridge is safe and stable.



(a) (b)

Fig. 10 – Temperature monitoring test results

Arch rings linear monitoring results

Monitoring results of arch rings elevation are shown in Figure 11. The figure shows the elevation data of the arch rings before and after the disassembly of the arch rings support. The largest elevation difference of the arch rings is at the 1-3# suspender section, the 1-2# suspender section and the 2-3# suspender section in turn, of which the difference of the 1-2# suspender is 1.4cm at most, followed by the 1-3# with 1.3 cm and the 2-3# with 1.2cm respectively. Generally speaking, the elevation of the arch rings changes little before and after the disassembly of the support, which meets the requirements of design and construction safety.

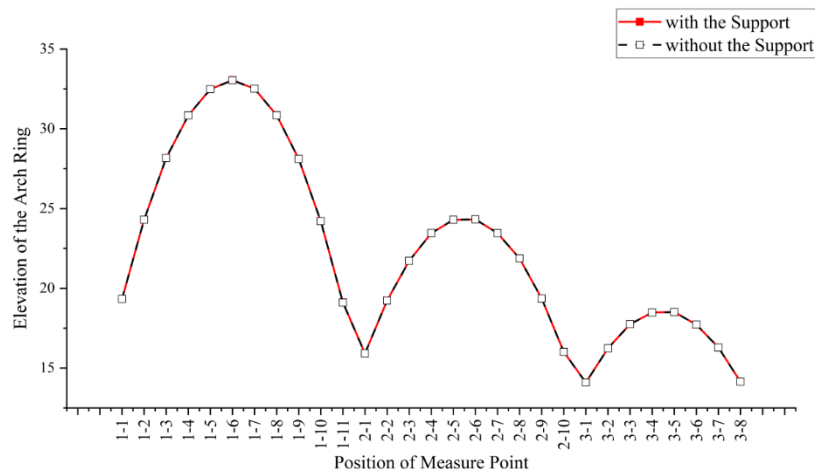


Fig. 11 – Monitoring results of arch rings elevation

Monitoring results of hangers' force

Comparison of measured hangers force and target force under bridge completion is shown in Figure 12. The hangers force line of the suspender is similar to the elevation curve of the arch rings, and it can be clearly seen that the column chart presents three arcs. The hanger force of D6 is the largest, reaching 824.8 kN, slightly less than the target force of 828.6 kN. The hanger force of the D29 is the smallest, only 325.1 kN, which is also smaller than the target cable force of 325.9 kN. In the second span, the measured force is slightly larger than the target force. But in general, there is minor division between the measured force and the designed force in the completed bridge.

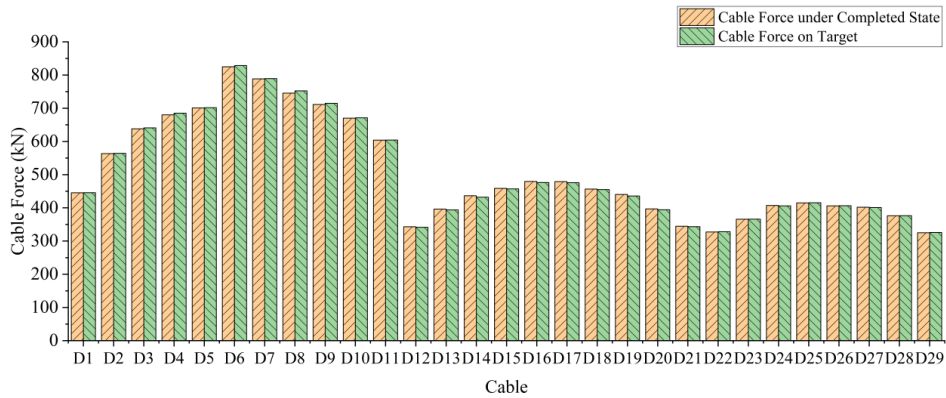


Fig. 12 – Monitoring results of hangers' force

LOAD TEST RESULTS

Static load test results

Girder deflection test results

Test results of main girder deflection are shown in Figure 13. From the direction of the deflection measurement points, the measured value reaches the maximum at N3 under working condition 1, which is 2.9 mm, lower than the theoretical value of 3.06 mm. The deflection curves under working conditions 2 and 4 decrease in turn in the direction of the transverse bridge under the test load, and reach the minimum deflection of 2.54 mm and 1.54 mm at N6, and the maximum deflection of 3.77 mm and 2.69 mm at N1, respectively. Under working condition 3, the measured deflection at N3 has a maximum value of 2.2 mm. The measured deflection values of the mid-span section of the main girder of the test holes are all less than the theoretical calculated values, and the deflection check coefficient is between 0.53 and 0.89, which indicates that the bearing capacity of the structure meets the design requirements. Besides, the residual deflection is less than 20%.

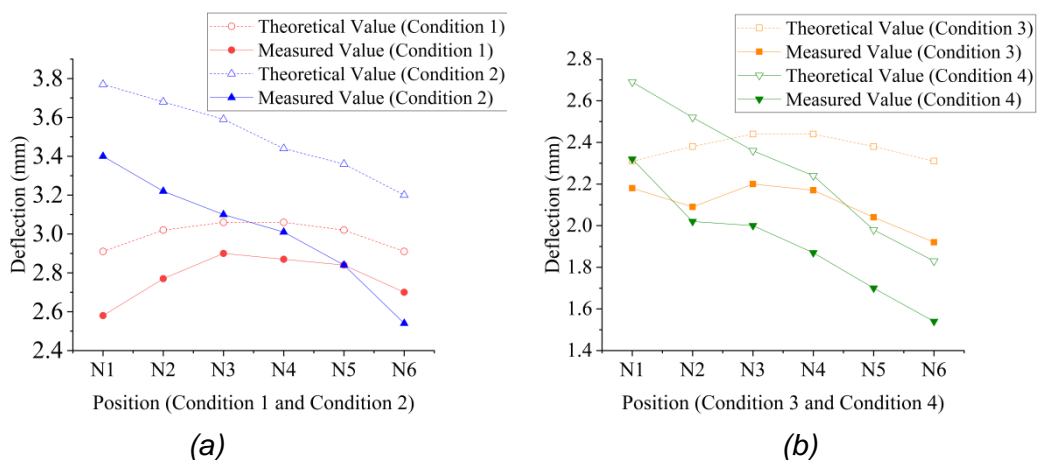


Fig. 13 – Comparison of measured and theoretical values of main girder deflection

Strain test results of girder

As shown in Figure 14, four curves represent the variation rule of main girder strain under four

working conditions. Under the load of test conditions 1 and 3, the transverse strain of the main girder presents a trapezoidal distribution. Under test condition 1, the measured values of M3 and M4 are the largest, which are 55 and 60 respectively, less than the theoretical value 86. Under working condition 3, the transverse strain of measuring points M3 and M4 is also larger than that of other measuring points upward of the main girder transverse bridge. However, the measured value is still less than the theoretical value. Under the four working conditions, the measured values of the transverse strain of the main girder are all less than the theoretical values. As a result, all tested girders are in the state of tension, which meets the designed requirements.

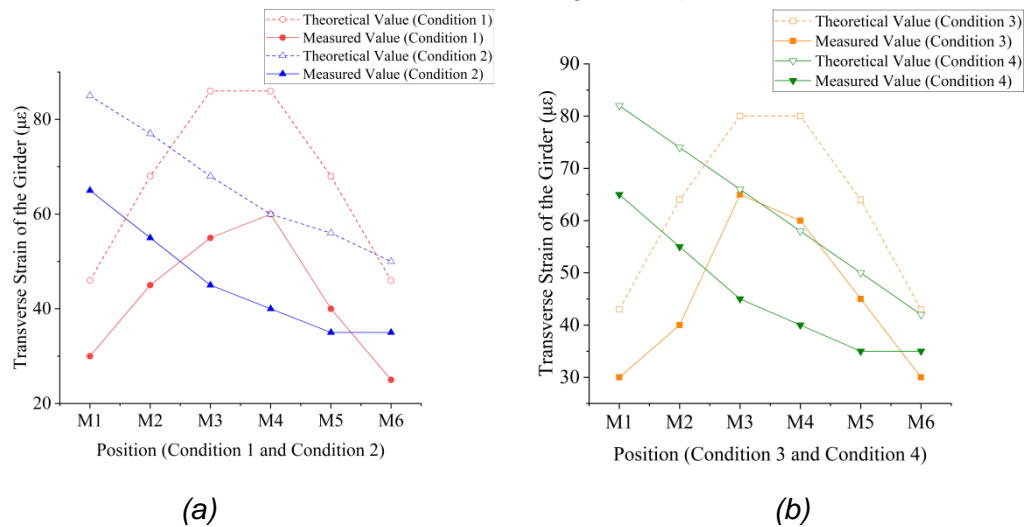


Fig. 14 – Comparison between measured and theoretical values of transverse strain of main girder

Test results of vertical strain of main girder are shown in Figure 15. The measured and theoretical values of M7~M12 are decreasing under the four working conditions. The maximum measured vertical strain of measuring point M7 under four working conditions is 30, 65, 35, 65, 65 respectively. Under working condition 1, the minimum vertical strain of the main girder is -60 of the measuring point M12, indicating that the measuring point is under pressure at this time. The strains the vertical measuring point is between -60 and 65 under the test condition 2. The measured minimum value of the measuring point M12 is -20, and the maximum value is 35 of the measuring point M7 in the test condition 3. Under the test condition 4, the measured minimum strain of M12 is -60, and the maximum strain is 65. Under the four test conditions, the measured transverse strains are less than the theoretical strains. Besides, the decline rate of test conditions 2 and 4 is greater than that of conditions 1 and 3.

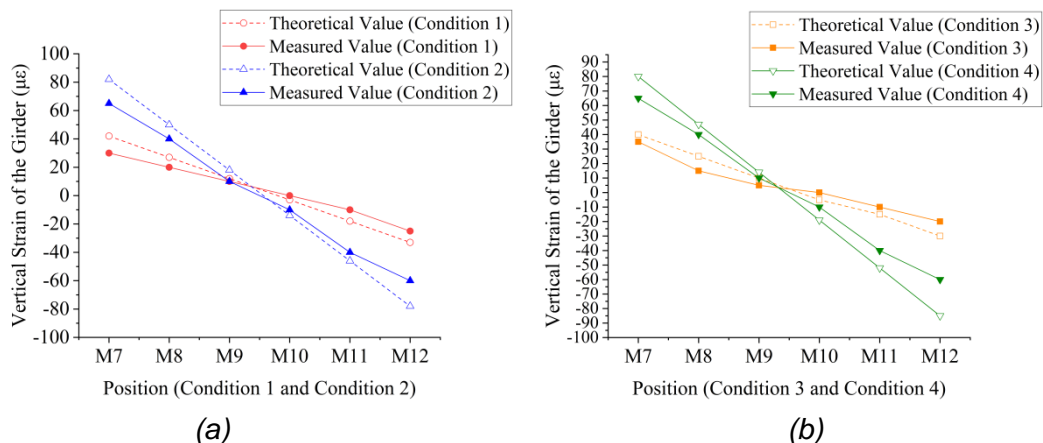


Fig. 15 – Comparison of measured and theoretical vertical strain values of main girder

Test results of hangers’ force

Test results of hangers’ force are shown in Table 4. Under test condition 2, the difference between the measured and theoretical values of D2 is the largest. Compared with the theoretical value of 93 kN, the measured value of D2 suspender is only 66 kN, and its difference is 27 kN. Meanwhile, the check coefficient of hangers’ force increment is 0.71. The second is the hanger force at position D2 under test conditions 1 and 3 respectively. In these two test conditions, the check coefficient at positions D1 and D2 is 0.73. Then the difference between the theoretical force and the measured force is 26 kN and 21 kN, respectively. In the whole static load test, the difference between the theoretical value and the measured value of the hanger force is obvious, but the increment check coefficient of the cable force at several measuring points is between 0.71 and 0.83, which achieves the designed standards.

Tab. 4 -Test Results of Suspender Force

Working Condition	Position	Theoretical Value (kN)	Measured Value (kN)	Testing Coefficients
Condition 1	D1	92	72	0.78
	D2	95	69	0.73
	D3	94	77	0.82
Condition 2	D1	90	75	0.83
	D2	93	66	0.71
	D3	92	74	0.8
Condition 3	D1	80	60	0.75
	D2	78	57	0.73
	D3	80	65	0.81
Condition 4	D1	77	58	0.75
	D2	81	60	0.74
	D3	80	66	0.83

Dynamic load test results

The test results of dynamic load test including pulsation test, 5 km/h, 10 km/h and 20 km/h are shown in Figure 16. The pulsation curve and frequency waveform are measured by velocity sensor on the deck of tied arch bridge. The third span natural vibration frequency was in 12.55 Hz~17.10 Hz. The measured frequency is all larger than the theoretical frequency of 10.93 Hz, which proves that the tied arch bridge has a adequate stiffness actually.

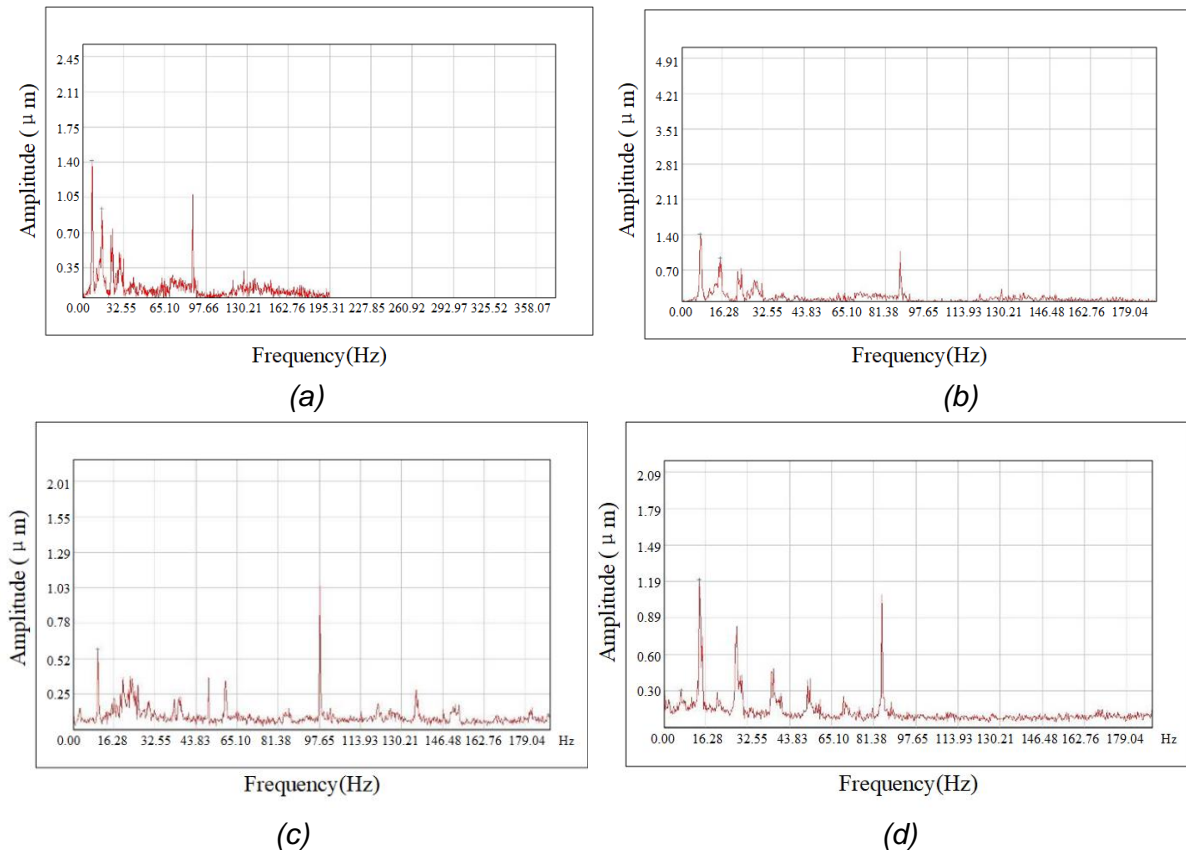


Fig. 16 – The test results of dynamic load tests:(a) Natural frequency spectrum of the second span of the west bridge in the pulsation test; (b) Natural spectrum diagram of bridge in the 5 km/h running test ($F = 14.63$ Hz); (c) Natural spectrum diagram of bridge in the 5 km/h running test ($F = 16.31$ Hz); (d) Natural spectrum diagram of bridge in the 5 km/h running test ($F = 17.10$ Hz)

CONCLUSION

- (1) The largest elevation difference of the arch rings is at the 1-3# suspender section, the 1-2# suspender section and the 2-3# suspender section in turn, of which the difference of the 1-2# suspender is 1.4cm at most, followed by the 1-3# with 1.3 cm and the 2-3# with 1.2cm respectively. The arch ring elevation changes little before and after the removal of the support, indicating that the weight of the main beam is borne by the derrick and the main beam.
- (2) The hangers force line of the suspender is similar to the elevation curve of the arch rings, and it can be clearly seen that the column chart presents three arcs. The hanger force of D6 is the largest, reaching 824.8 kN, slightly less than the target force of 828.6 kN. The hanger force of the D29 is the smallest, only 325.1 kN, which is also smaller than the target cable force of 325.9 kN. In the second span, the measured force is slightly larger than the target force. There is minor division between the measured force and the designed force in the completed bridge.
- (3) Measured strain of the bridge under the test conditions is basically linear in the direction of the beam height, indicating that the structure basically conforms to the assumption of the plane section when working. The measured deflection of the mid-span girder is always less than the calculation values, and the deflection is between 1.54~3.40 mm, indicated that the stiffness of the box-girders meets the designed standards. Natural vibration frequency of the tied arch bridge was

measured between 12.55 Hz and 19.55 Hz by the pulsation test. At the same time, the measured data are all greater than the theoretical value of 10.93 Hz. The dynamic load test shows that the stiffness meets the requirements. The load tests have achieved an expected purpose.

REFERENCE

- [1] He M, Fu X, Chen S. Evaluation of bearing capacity of reinforced concrete box ribbed arch bridge based on static load test[J]. E3S Web of Conferences, 2021, 233(3):01024.
- [2] R Ceravolo, Coletta G, Lenticchia E, et al. In-Operation Experimental Modal Analysis of a Three Span Open-Spandrel RC Arch Bridge[M]. 2020.
- [3] Kolla A, Kurapati R, Meka S, et al. Health Assessment and Modal Analysis of Historical Masonry Arch Bridge[M]. 2021.
- [4] Benedetti A, Tarozzi M, Pignagnoli G, et al. Dynamic Investigation and Short-Monitoring of an Historic Multi-span Masonry Arch Bridge[M]. 2020.
- [5] Zhou Y. The suspender construction error and control of a through tube tied arch bridge[J]. Shanxi Architecture, 2010.
- [6] Ammendolea D, Greco F, Blasi P N, et al. Strategies to improve the structural integrity of tied-arch bridges affected by instability phenomena[J]. Procedia Structural Integrity, 2020, 25:454-464.
- [7] Zong Z H, Jaishi B, Ge J P, et al. Dynamic analysis of a half-through concrete-filled steel tubular arch bridge[J]. Engineering Structures, 2005, 27(1):3-15.
- [8] Chen H, Dong J H. Practical Formulae of Vibration Method for Suspender Tension Measure on Half-through and Through Arch Bridge[J]. China Journal of Highway & Transport, 2007, 20(3):66-70.
- [9] Jing-xian, SHI, Zhuo-yin, et al. Simulation Calculation and Monitoring of Deformation of Concrete-Filled Steel Tube Arch Bridge[C]// 2018.
- [10] Nonaka T, Ali A. DYNAMIC RESPONSE OF HALF-THROUGH STEEL ARCH BRIDGE USING FIBER MODEL[J]. Journal of Bridge Engineering, 2001, 6(6):482-488.
- [11] Li J B, Ge S J, Chen H. Seismic behavior analysis of a 5-span continuous half-through CFST arch bridge[J]. World Information on Earthquake Engineering, 2005.
- [12] Shao Y, Sun Z G, Chen Y F, et al. Impact effect analysis for hangers of half-through arch bridge by vehicle-bridge coupling[J]. Structural Monitoring and Maintenance, 2015, 2(1):65-75.
- [13] Wang H. Study on deformation monitoring of continuous through concrete-filled steel tube arch bridge[J]. IOP Conference Series: Materials Science and Engineering, 2019, 592(1):012005 (7pp).
- [14] Meixedo A G, Ribeiro D, Santos J P, et al. Progressive numerical model validation of a bowstring-arch railway bridge based on a structural health monitoring system[J]. Journal of Civil Structural Health Monitoring, 2021.
- [15] Lu W, Li J, Yu L, et al. Force Analysis of Arch rings of Half-Through Irregular CFST Tied Arch Bridge during Construction Stage[J]. International Journal of Critical Infrastructures, 2021, 17(4):1.
- [16] Yao G W, Chao Y, Wu H J, et al. Construction Control of Hoisting and Installation of Arch rings of a Half-Through CFST Stiff Skeleton Arch Bridge[J]. Bridge Construction, 2017, 47(5):107-111.
- [17] Guan J W, Wang C J. Analysis of In-pipe Concrete Grouting Process for Arch ringss in Half-through Concrete-filled Steel Tubular Arch Bridge[J]. Western China Communications Science & Technology, 2018.
- [18] Farahmand-Tabar S, Barghian M. Seismic assessment of a cable-stayed arch bridge under three-component orthotropic earthquake excitation[J]. Advances in Structural Engineering, 2020, 24(2):227–242.
- [19] Elewa M. Numerical Investigation on the Behavior of Skewed Concrete Tied Arch Bridges[M]. 2020.
- [20] Senatore G, Reksowardojo A P. Force and Shape Control Strategies for Minimum Energy Adaptive Structures[J]. Frontiers in Built Environment, 2020, 6:105.

- [21] T Forgács, Sarhosis V , S Dány. Shakedown and dynamic behaviour of masonry arch railway bridges[J]. Engineering Structures, 2020, 228.
- [22] Ma L. Study on Stress Properties and Optimization of Critical Nodes of Long-span Steel Truss Arch Bridge[J]. Urban Roads Bridges & Flood Control, 2018.
- [23] Karieta V. THE ANALYSIS OF RATIONAL COMPONENT PARAMETERS FOR STRESS RIBBON THROUGH STEEL ARCH FOOTBRIDGES[J]. Engineering Structures and Technologies, 2018, 10(2):72-77.